D-meson production in e^+e^- annihilation at $E_{c.m.}$ between 3.8 and 6.7 GeV

M. W. Coles,[a] G. S. Abrams, C. A. Blocker,[b] A. Blondel, W. C. Carithers, W. Chinowsky, S. Cooper,[c]
W. E. Dieterle, J. B. Dillon, M. W. Eaton, G. Gidal, G. Goldhaber, A. D. Johnson, J. A. Kadyk,
A. J. Lankford, R. E. Millikan, M. E. Nelson, C. Y. Pang, J. F. Patrick, J. Strait, G. H. Trilling,
E. N. Vella, and I. Videau[d]

Lawrence Berkeley Laboratory and Department of Physics, University of California,
Berkeley, California 94720

M. S. Alam,[e] A. Boyarski, M. Breidenbach, D. L. Burke, J. Dorenbosch,[f] J. M. Dorfan, G. J. Feldman,
M. E. B. Franklin, G. Hanson, K. A. Hayes,[f] T. Himel,[f] D. G. Hitlin,[g]R. Hollebeek, W. Innes, J. Jaros,
P. Jenni,[f] R. R. Larsen, V. Luth, M. L. Perl, B. Richter, A. Roussarie,[h] D. L. Scharre,
R. H. Schindler,[f] R. F. Schwitters,[b] J. L. Siegrist, H. Taureg,[f] M. Tonutti,[i] R. A. Vidal,
J. M. Weiss, and H. Zaccone[h]

Stanford Linear Accelerator Center, Stanford University, Stanford, California 94305
(Received 2 June 1982)

The Mark II detector at SPEAR has been used to study D-meson production in e^+e^- annihilation at center-of-mass energies between 3.8 and 6.7 GeV. The neutral and charged D mesons are identified from their $K^\mp\pi^\pm$ and $K^\mp\pi^\pm\pi^\pm$ decay modes. Measurements of R_D and of the inclusive differential cross section $s\,d\sigma/dz$ are presented. The quasi-two-body cross sections $\sigma_{D\bar{D}}$, $\sigma_{D^*\bar{D}}$, and $\sigma_{D^*\bar{D}^*}$ are derived from an overall fit to the D recoil spectra. No evidence was found for the associated production of charmed mesons and charmed baryons.

I. INTRODUCTION

One of the most useful indicators of new phenomena in e^+e^- annihilation has been the energy dependence of R, the ratio of the hadronic to muon-pair cross sections. At energies above the prominent ψ and ψ' peaks, R exhibits a complex energy dependence associated with the production of charmed particles. The production of charmed mesons has been studied at the ψ'' and higher energies. These studies[1,2] have determined the mass of the charged and neutral D and D^*, their spins,[3,4] D and D^* branching fractions[5] to various final states, and production cross sections[6] at various center-of-mass energies. In this paper we present the results of a study of D and D^* production at center-of-mass energies between 3.8 and 6.7 GeV using the SLAC-LBL Mark II detector at the storage ring SPEAR.

Our measurements are presented in the following way. In Sec. II we summarize the relevant features of the detector. In Sec. III, we discuss the measurement of the energy dependence of inclusive neutral- and charged-D production cross sections. In Sec. IV we present more detailed results on the inclusive momentum spectrum of D's at a center-of-mass energy of 5.2 GeV, where substantial

statistics were accumulated. In Sec. V we give an upper limit for the cross section for the associated production process $e^+e^-\rightarrow\Lambda_c\bar{D}N$. Section VI discusses the "resonance region" in R between roughly 3.8 and 4.4 GeV. The energy dependence of the production cross sections for the exclusive reactions $e^+e^-\rightarrow D\bar{D}$, $e^+e^-\rightarrow D^*\bar{D}$ or $\bar{D}^*D$, and $e^+e^-\rightarrow D^*\bar{D}^*$ is discussed, and measurements of the branching fractions for the decays of charged and neutral D^*'s to pions or photons are presented. Finally, the energy dependence of these exclusive cross sections is compared to that dependence
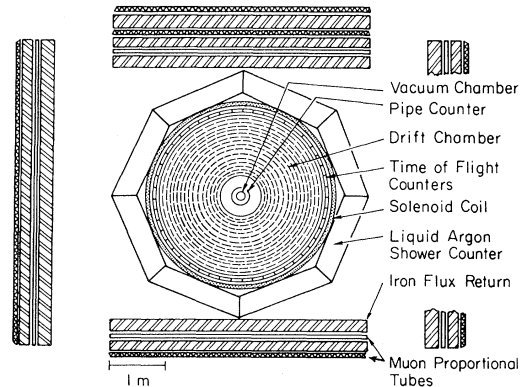

FIG. 1. Cross-sectional view of the Mark II detector.

Labels: Vacuum Chamber, Pipe Counter, Drift Chamber, Time of Flight Counters, Solenoid Coil, Liquid Argon Shower Counter, Iron Flux Return, Muon Proportional Tubes, 1 m

predicted theoretically by the $q\bar{q}$ potential model of Eichten *et al.*

II. EXPERIMENTAL APPARATUS

The Mark II detector (see Fig. 1) has been described in detail elsewhere.[7,8] We concentrate on relevant features. Starting at the interaction region a particle first traverses a corrugated-stainless-steel vacuum pipe and a set of trigger scintillation counters, which together comprise about 0.05 radiation lengths of material. It then traverses a 16-layer drift chamber, a hodoscope of 48 time-of-flight counters, and an aluminum solenoidal coil which produces a 0.42-T axial magnetic field. Beyond the coil are eight lead—liquid-argon electromagnetic shower-counter modules and two or three layers of muon identifiers, each layer consisting of 23 to 30 cm of iron and a set of proportional tubes.

Charged tracks are reconstructed from signals in the 16 cylindrical-drift-chamber layers. The azimuthal coordinates of charged tracks are measured to an rms accuracy of approximately 220 μm at each layer. The polar coordinates are determined from the ten "stereo" layers oriented at approximately $\pm 3°$ to the beam axis. When a track can be constrained to pass through the vertex, the charged-particle rms momentum resolution is $\delta p/p = [(0.015)^2 + (0.005p)^2]^{1/2}$ where p is the transverse momentum in GeV/c. Without this constraint the coefficient of the momentum-dependent term is doubled. Tracks are required to come within 1 cm radially and within ± 10 cm longitudinally of the measured beam crossing point. To ensure more uniform detection efficiency and optimum momentum resolution, tracks passing this selection were required to have $|\cos\Theta| < 0.75$, where Θ is the polar angle relative to the beam axis at the production vertex. Measured momenta are corrected for dE/dx losses in material traversed before entering the drift chamber.

The time-of-flight (TOF) scintillation counters which surround the drift chamber provide timing information over 75% of 4π sr. Each TOF counter is a 2.54-cm-thick Pilot F scintillator, 3.44 m long, and is viewed on each end by an Amperex XP 2230 photomultiplier tube. The system was calibrated using isochronous light pulses from a nitrogen flashtube, brought to the center of each counter through 10-m-long fibers. Signals from the tubes are fed to 12-bit time-to-digital convert-

ers (TDC's) and analog-to-digital converters (ADC's), the latter allowing a pulse-height correction to be made. These slewing corrections are calculated off-line from Bhabha-scattered electrons and allow us to obtain a system resolution of 315 ps for hadrons.

The lead—liquid-argon shower-counter modules which surround the solenoid are used to detect photons and identify high-energy electrons. The modules are approximately 14 radiation lengths in depth, provide almost full 2π azimuthal coverage about the beam direction, and cover 64% of 4π sr. The rms energy resolution for photons above 500 MeV in the calorimeter is approximately $12\%/\sqrt{E}$ (GeV), but deteriorates somewhat at lower energies due to the effect of the coil. The angular resolution for photons is approximately 8 mrad.

The detector trigger employs a track-finding hardware processor which requires at least one track to traverse the entire drift chamber and an additional track to cross at least three of the five inner layers. All D decays that we investigate have at least two charged tracks which traverse the entire chamber.

The luminosity of the data sample is monitored by a pair of small-angle scintillators and shower counters. These counters are positioned at 22 mrad from the beam axis, and identify Bhabha-scattered electrons. The counters are calibrated against larger-angle Bhabha events measured in the fiducial volume of the drift chamber and lead—liquid-argon calorimeter.

D mesons used in this analysis were observed in the detector as peaks in the invariant-mass spectra of the decay modes $D^0 \rightarrow K^-\pi^+$ and $\bar{D}^0 \rightarrow K^+\pi^-$, and $D^{\pm} \rightarrow K^{\mp}\pi^{\pm}\pi^{\pm}$. These modes were chosen because of their relatively large branching fractions and because the invariant-mass distributions had a better ratio of signal to background than other decay channels.

To detect D's which decay in this way, we relied on the ability of the time-of-flight counters to discriminate between charged pions and charged kaons. A π-K separation of greater than 1σ time difference was possible for tracks with a momentum less than 1.35 GeV/c. Similarly, π-p and K-p separation was achieved for particle momenta less than 2.0 GeV/c. Each track was assigned three weights corresponding to its possible identity as a pion, kaon, or proton (antiproton). Each weight was proportional to the Gaussian probability that if the particle had the assumed identity, its mea-

sured flight time would have deviated from the predicted flight times as much as observed. The normalization was such that the sum of all weights corresponding to a given track was unity. A particle was considered to be a proton if it had a proton weight greater than 0.9, it was called a kaon if it had a kaon weight greater than 0.5, and it was called a pion otherwise. Particles also were considered to be pions if there was no time-of-flight information available for them.

We eliminate positively identified leptons as follows. A second set of time-of-flight weights was formed to discriminate between electrons (or positrons) and pions if the momentum of the particle was less than 300 MeV/c. Tracks with an electron weight greater than 0.8 were taken to be electrons. At momenta above 300 MeV/c, electron-pion discrimination was based on the longitudinal distribution of energy deposited in the liquid-argon shower counters.[9] Above 800 MeV/c, muons were distinguishable in the muon range counters.

III. THE INCLUSIVE D PRODUCTION CROSS SECTION

We have measured the ratio of the inclusive D-meson production cross section to the theoretical muon-pair production cross section

$$R_D = \frac{\sigma(D^+) + \sigma(D^-) + \sigma(D^0) + \sigma(\bar{D}^0)}{\sigma(\mu^+\mu^-)}$$

for center-of-mass energies between 3.9 and 6.7 GeV.

In this analysis we determine a model-independent efficiency for detection of D mesons. A previous measurement[10] has shown that D-meson production in e^+e^- annihilation is consistent with being entirely two-body or quasi-two-body below a center-of-mass energy of 4.4 GeV and more complex above this energy. For this reason we have determined momentum-dependent detection efficiencies and studied their sensitivity to the details of these various production mechanisms.

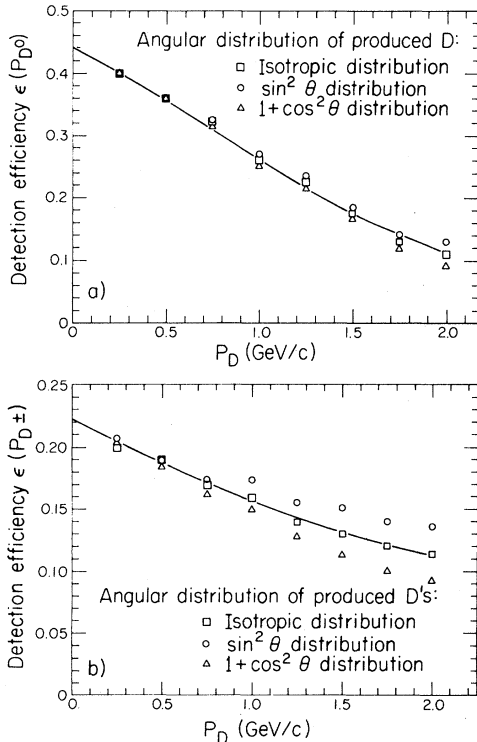The detection efficiencies were determined by using a Monte Carlo program to generate D's at vari-

FIG. 2. Momentum-dependent detection efficiencies for (a) $D^0 \rightarrow K^-\pi^+$, (b) $D^+ \rightarrow K^-\pi^+\pi^+$. Both diagrams show the effects of angular distribution in the production angle of a D with respect to the beam direction. The solid lines are our parametrizations of the isotropic production detection efficiencies.
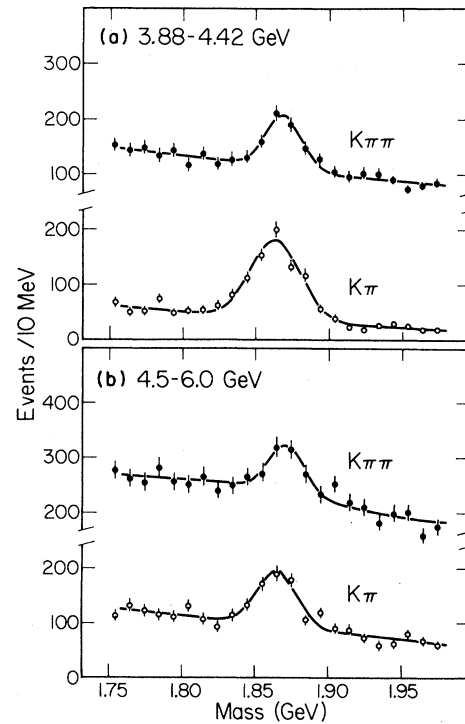

FIG. 3. The $K^\mp\pi^\pm$ and $K^\mp\pi^\pm\pi^\pm$ invariant-mass distributions for accumulated data at center-of-mass energies (a) between 3.88 and 4.42 GeV, and (b) between 4.5 and 6.0 GeV. The curves are the results of a fit to a Gaussian plus a polynomial background.

TABLE I. Measured R_D for each energy interval.

Energy (GeV)	Luminosity (nb⁻¹)	No. of events $D^{\pm}$	No. of events D^0	$\sigma_{\pm}B(D^+\to K^-\pi^+\pi^+)$ (nb)	$\sigma_0B(D^0\to K^-\pi^+)$ (nb)	$\sigma_{\pm}$ (nb)	σ_0 (nb)	R_D
3.88−4.02	374	18± 9	23± 6	0.25±0.13	0.17±0.04	4.0±2.1	5.7±1.3	1.7±0.4
4.02−4.15	906	41±12	152±15	0.29±0.08	0.54±0.06	4.6±1.3	18.0±2.0	4.3±0.5
4.16	1248	42±12	128±14	0.19±0.06	0.30±0.03	3.0±1.0	10.0±1.0	2.6±0.3
4.15−4.20	342	17± 7	45± 8	0.27±0.12	0.38±0.07	4.3±1.9	12.7±2.3	3.4±0.6
4.20−4.30	672	25± 9	40±10	0.23±0.06	0.17±0.04	3.7±1.0	5.7±1.3	2.0±0.4
4.30−4.40	221	26± 8	19± 9	0.80±0.25	0.34±0.15	12.7±4.0	11.3±5.0	5.3±1.4
4.40−4.42	1315	54±16	160±18	0.25±0.07	0.40±0.05	4.0±1.1	13.3±1.7	3.9±0.4
4.50−4.85	1565	65±17	65±15	0.23±0.06	0.13±0.03	3.7±1.0	4.3±1.0	2.0±0.4
4.85−5.20	1655	57±18	74±17	0.27±0.09	0.22±0.05	4.3±1.4	7.3±1.7	3.3±0.6
5.20	5110	118±33	241±31	0.15±0.04	0.18±0.03	2.4±0.6	6.0±1.0	2.6±0.4
5.20−6.00	753	8^{+12}_{-4}	30±10	$0.08^{+0.09}_{-0.04}$	0.19±0.05	$1.3^{+1.4}_{-0.6}$	6.3±1.7	$2.8^{+0.8}_{-0.6}$
6.5 −6.70	3650	44±16	54±17	0.10±0.03	0.07±0.02	1.6±0.5	2.3±0.7	2.0±0.5

ous momenta. The Monte Carlo program is designed to represent the properties of the detector as closely as possible. The D's were generated both in an isotropic angular distribution and in the distributions $dN/d\Omega \sim 1\pm\cos^2\Theta$ where Θ is the angle between the D momentum and e^+ beam. The D's were then allowed to decay, and the pions and kaons resulting from these decays were propagated through the detector. The pions and kaons were also allowed to decay, and tracks were reconstructed and selected to determine the detection efficiencies. The momentum dependence of the neutral- and charged-D detection efficiencies is shown in Fig. 2. Even though Fig. 2 indicates a difference of nearly 25% between the isotropic and anisotropic charged-D detection efficiencies at 2 GeV/c, it was found from the substantial statistics accumulated at 5.2 GeV that the momentum distribution of D's is peaked at low momenta. That behavior minimizes this source of uncertainty.

In Fig. 3 we show the $K^{\mp}\pi^{\pm}$ and $K^{\mp}\pi^{\pm}\pi^{\pm}$ invariant-mass distributions in the D-meson region for the accumulated data divided into two center-of-mass energy regions: 3.88−4.42 GeV [Fig. 3(a)] and 4.5−6.0 GeV [Fig. 3(b)]. The widths (σ) obtained from the fits to a Gaussian plus a polynomial background are 17.2±1.7 MeV $(K\pi)$, 12.3±1.5 MeV $(K\pi\pi)$ at the lower energies and 13.8±2.1 MeV $(K\pi)$, 12.4±3.3 MeV $(K\pi\pi)$ at the higher energies. The widths determined from the Monte Carlo program (17 MeV for $K\pi$, 15 MeV for $K\pi\pi$) are consistent with these measurements and are almost independent of the D-meson momentum.

We determined the amount of D production by analyzing our data in the following way. The numbers of charged and neutral D's produced at a particular center-of-mass energy were determined from $K^{\mp}\pi^{\pm}$ and $K^{\mp}\pi^{\pm}\pi^{\pm}$ invariant-mass distributions in various momentum bins. These invariant-mass distributions for each momentum bin were fit to a Gaussian distribution plus a quadratic background. The center of the Gaussian was fixed at the known D mass, and its width was fixed to be the resolution width determined by the Monte Carlo simulation.

The number of produced D's was determined by dividing the detected number of D's (the results of the invariant-mass fits) by the detection efficiency for isotropic production. The detection efficiency was evaluated at the center of the D momentum bin. The Mark II experiment has measured[1] the $D^0\to K^-\pi^+$ branching fraction and determined it

to be 0.03 ± 0.006. The $D^+ \rightarrow K^-\pi^+\pi^+$ branching ratio was determined to be 0.063 ± 0.011. These values were used to obtain the total numbers of produced D's.

Systematic sources of uncertainty in the numbers of produced charged and neutral D's are any deviation from the assumed isotropic production angular distribution and any variation of the detection efficiency over the range of each momentum slice. These sources of error together produced a systematic uncertainty of less than 12% in the determination of the total number of neutral D's produced and uncertainty of, in general, less than 17% in the amount of charged-D production. To calculate the inclusive D production cross section from the number of produced D's, luminosities[11] based on wide-angle Bhabha scattering were used. These luminosities have a systematic error of 6% which is negligible in relation to the other statistical and systematic sources of uncertainty.

The results are given in Table I and plotted in Fig. 4. In the region below 4.5 GeV, we observe structure in the total R_D. Most of this structure comes from the excess of D^0 over D^+, which is expected if most of the D's come from D^* decay. The data were radiatively corrected according to the method of Bonneau and Martin.[12] These corrections are at most 15% near the 4 GeV structure and less than 5% elsewhere. In Fig. 5 we compare the Mark II measurement of R (the usual ratio of total hadronic cross section to muon-pair cross section),[11] with the sum of our measured value of $R_D/2$ and 2.5. The number 2.5 (±0.25) is an estimate of the contribution from light (u,d,s) quarks based on the various measured values of R below charm threshold.[13] Note that because D's are produced in pairs, R_D double counts the fraction of events containing D's. From the comparison in Fig. 5, we see that D production alone accounts for almost all of the charm contribution to R up to at least 6 GeV. The structure observed in R_D between 3.8 and 4.5 GeV is discussed in Sec. VI.

One can use Fig. 5 to set limits on the production cross section for the F meson and for charmed baryons at 5.2 GeV. We assume that the light-quark (u,d,s) contribution to R is 2.5, independent of c.m. energy, and that within statistical errors R is equal to $R_D/2+2.5$. The systematic errors (roughly 20% on R_D, 10% on the light-quark contribution and 10% on R itself) then give a limit of one-half unit of R for the pair production cross section of F mesons or charmed baryons. This is
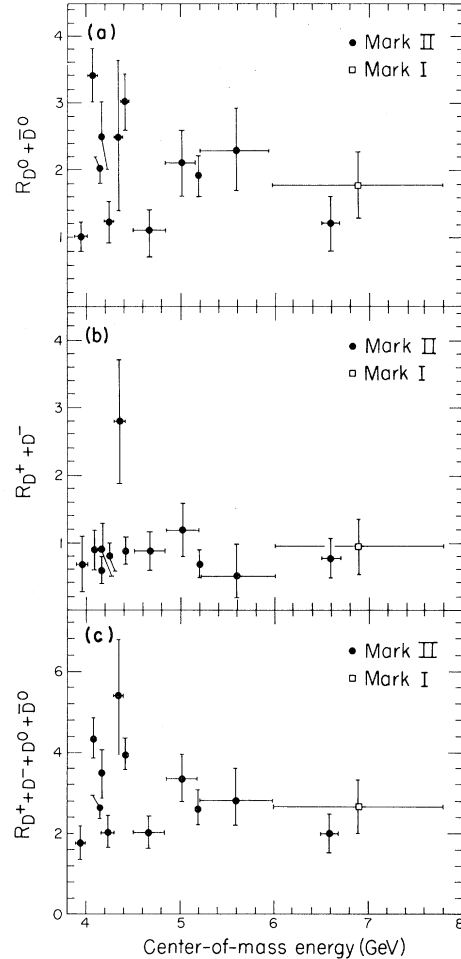

FIG. 4. The energy dependence of the inclusive D production cross section divided by the muon-pair production cross section for (a) neutral D's alone, (b) charged D's alone, and (c) charged and neutral D's together. A data point from Ref. 17 (Mark I) is also shown.
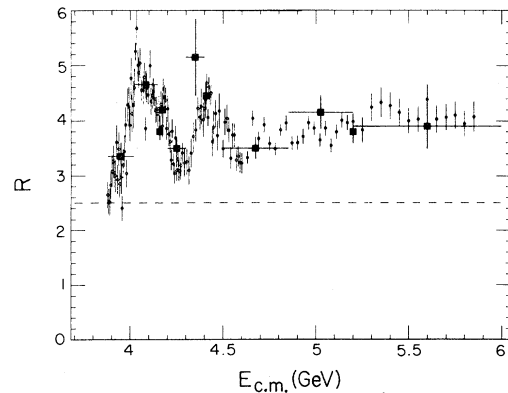

FIG. 5. Comparison of $R_D/2+2.5$ (■) to the total hadron production R (♦). 2.5 is the average measured value of R below charm threshold.

consistent with the Mark II measurement[14] of $\Delta R \approx 0.3$ for charmed baryons above 5 GeV.

IV. INCLUSIVE *D* PRODUCTION AT 5.2 GeV

The availability of a large data sample at 5.2 GeV made it feasible to investigate in some detail the charm production characteristics at that center-of-mass energy. In particular, we measured the differential distribution in the scaling variable z, the ratio of total energy of the *D* meson to the beam energy. The kinematic limits imposed by the large *D* mass are that $0.72 \le z \le 1$.

We determined the quantity $s\, d\sigma/dz$ in the same way as in Sec. III, fitting $K^\pm \pi^\mp$ and $K^\pm \pi^\pm \pi^\pm$ invariant-mass spectra within z bins of 0.05 units width to Gaussian distributions of fixed mean and width, plus quadratic backgrounds. As usual, s is the square of the center-of-mass energy. The detection efficiencies of Fig. 2 and the branching fractions measured in the Mark II detector for $D^0 \rightarrow K^- \pi^+$ and $D^+ \rightarrow K^- \pi^+ \pi^+$ were then used to determine $s\, d\sigma/dz$. The individual fits are shown in Figs. 6 and 7 and the results are shown in Fig. 8.

It is apparent that the quasi-two-body production processes $D\bar{D}$, $D^*\bar{D} + \bar{D}^*D$, and $D^*\bar{D}^*$ are not

FIG. 7. Invariant-mass spectra for $K^\mp \pi^\pm \pi^\pm$ combinations for six regions of $z = 2E_D/\sqrt{s}$. The lines are our fits to the expected $D^+ \rightarrow K^- \pi^+ \pi^+$ mass spectra and are described in the text.
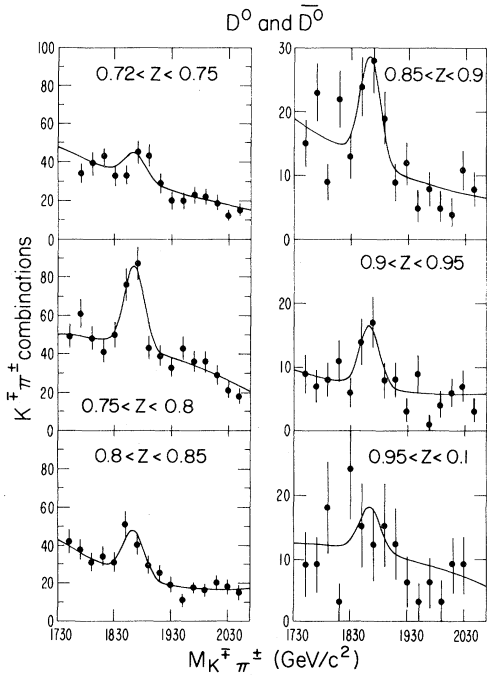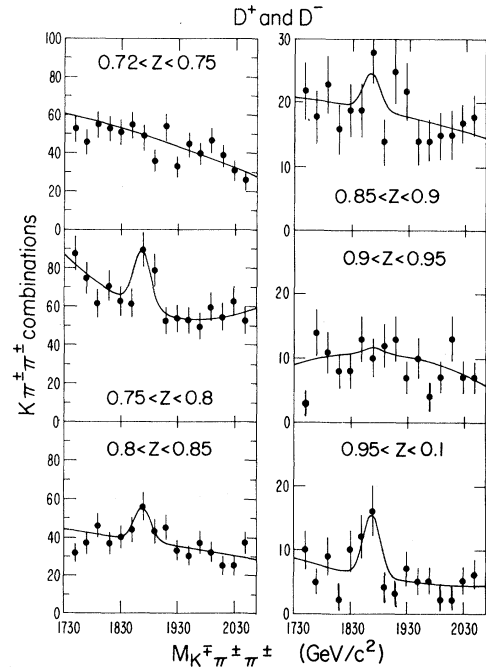
FIG. 6. Invariant-mass spectra for $K^\pm \pi^\mp$ combinations for 6 regions of $z = 2E_D/\sqrt{s}$. The lines are our fits to the expected $D^0 \rightarrow K^- \pi^+$ mass spectra and are described in the text.
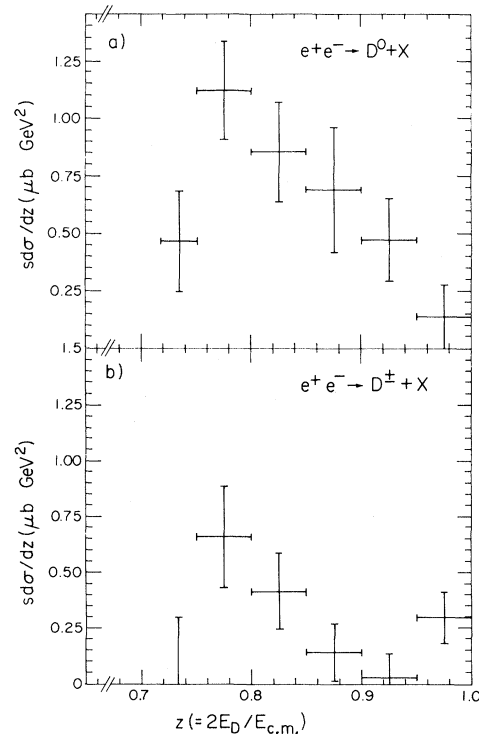
FIG. 8. The differential scaling cross section $s\, d\sigma/dz$ measured at a center-of-mass energy of 5.2 GeV for (a) neutral *D*'s and (b) charged *D*'s.

the dominant sources of D's at 5.2 GeV, since for such processes D's must have $z > 0.93$. The data of Fig. 8 indicate that less than 35% (90% confidence level) of $D^{\pm}$ production and less than 20% (90% confidence level) of D^0 production occurs this way.[15]

Figure 9 compares the distribution in $s\, d\sigma/dz$ observed for D^0 production at 5.2 GeV with the same quantity observed in e^+e^- production of $\pi^{\pm}$ and K_s^0 between 6.1 and 7.6 GeV.[16] Apart from the lowest- and highest-z bins, the slope of the D^0 spectrum has a value consistent with that observed for $\pi^{\pm}$ and K_s^0.

We have parametrized the D^0 spectrum in the form $s\, d\sigma/dz = A(1-z)^n$, and, ignoring the threshold bin, obtained $n = 0.9 \pm 0.4$. This value of n is in agreement with the previously reported[17] value of $0.76^{+0.45}_{-0.33}$ obtained by the Mark I experiment at a center-of-mass energy of 7.0 GeV. Since 5.2 GeV is rather close to $D\bar{D}$ threshold this distribution is severely constrained by kinematic effects and is thus not expected to accurately reflect the D fragmentation function at asymptotic energies.

V. ASSOCIATED PRODUCTION OF CHARMED BARYONS AND CHARMED MESONS

We have previously reported[14] the observation of inclusive charmed baryon (Λ_c) production in e^+e^- annihilation at 5.2 GeV. At 5.2 GeV, it is kinematically possible for the reactions $e^+e^- \rightarrow \Lambda_c \bar{D}^0 \bar{p}$ and $e^+e^- \rightarrow \Lambda_c D^- \bar{n}$ (or the charge conjugate states) to occur. The identification of a D meson and a proton or antiproton in the same event would prove the existence of one of these reactions as the threshold for $e^+e^- \rightarrow p\bar{p}D\bar{D}$ is about 5.6 GeV.

Two methods were used to search for these associated production processes. The first method required the detection of a D and the directly produced proton or antiproton, while the second method required the detection of the D and a proton from the decay of the charmed baryon.

To employ the first method, the effective mass recoiling against the detected $\bar{D}^0\bar{p}$ system (or its charge conjugate) was calculated. Such a system was defined as a $K^{\mp}\pi^{\pm}$ or $K^{\mp}\pi^{\pm}\pi^{\pm}\pi^{\mp}$ mass combination in the range 1.82 to 1.90 GeV/c^2 plus a particle identified by time of flight as being a p or $\bar{p}$. Only 13 such events were observed in the data sample of 5150 nb^{-1}, and of these 13 events, none
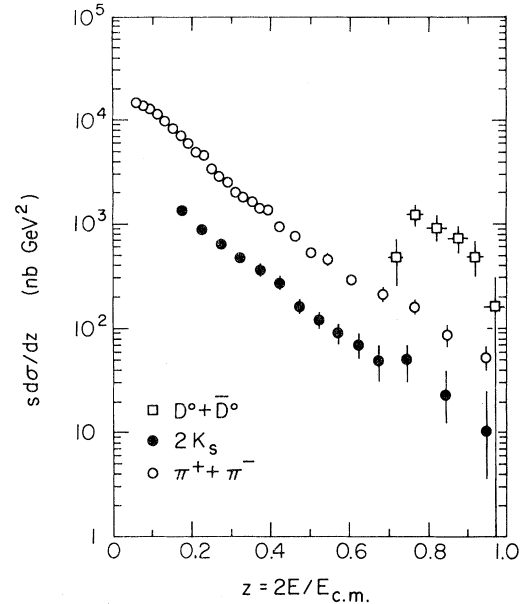

FIG. 9. Comparison of the differential scaling cross section $s\, d\sigma/dz$ for neutral D's produced at a center-of-mass energy of 5.2 GeV (Mark II) to that observed for charged pions and neutral kaons produced between 6.1 and 7.8 GeV (Mark I).

were observed to have a missing mass within 200 MeV/c^2 of the Λ_c mass[14] (2.284 GeV/c^2). This gives a limit on associated production of less than 0.4 nb (0.12 units of R) at the 90% confidence level.

In the second method for determining the existence of associated production, events were counted which contained a p and a $\bar{D}$ or a $\bar{p}$ and a D. The D was observed through the decays $D^0 \rightarrow K^{\mp}\pi^{\pm}$, $K^{\mp}\pi^{\pm}\pi^{\mp}\pi^{\pm}$, and $D^{\pm} \rightarrow K^{\mp}\pi^{\pm}\pi^{\pm}$. Events were labeled as having a D if the invariant mass of the K and π's was between 1.82 and 1.90 GeV/c^2. A background subtraction was made using invariant-mass combinations in the range of 1.65 to 1.69 GeV/c^2 or in the range between 2.03 and 2.07 GeV/c^2. Events in both the signal and the sidebands were required to have a p or $\bar{p}$ which was identified by time of flight with proton weight > 0.9. Sixteen such events were found containing a p or $\bar{p}$ in the signal region and 17 such events were found in the sidebands, leaving no evidence for associated production after background subtraction. From the branching ratios[1,18] for D decay to $K^-\pi^+$, $K^+\pi^-\pi^+\pi^-$, and $K^-\pi^+\pi^+$, and an isospin statistical model estimate that the fraction of Λ_c decays that lead to a proton is 0.6, an upper limit on associated production is estimated to be 0.4 nb, the same as for the first method.

VI. EXCLUSIVE CHANNELS
IN *D*-MESON PRODUCTION

In the 4-GeV region, three *D* production modes have been observed[10]:

(1) $e^+e^- \rightarrow D\bar{D}$,

(2) $e^+e^- \rightarrow D^*\bar{D}$ or $\bar{D}^*D$,

(3) $e^+e^- \rightarrow D^*\bar{D}^*$.

With the same data sample as in Sec. III, the relative rates of production of these three channels were measured at center-of-mass energies between 3.9 and 4.3 GeV. For the analysis of the exclusive channels, an event was said to be a *D* candidate if the $K^\mp \pi^\pm$ or $K^\mp \pi^\pm \pi^\pm$ invariant mass was between 1.82 and 1.90 GeV/c^2.

Because of the limited data sample available and the small branching fractions for $D^0 \rightarrow K^- \pi^+$ and $D^+ \rightarrow K^- \pi^+ \pi^+$, at most one *D* meson was detected in each event containing charm. To establish which of the three reactions was the mechanism for production of a particular *D*, the recoil effective mass opposite the *D* was calculated. If the *D* is directly produced, rather than the result of a *D** decay, the observed recoil-mass spectrum should be populated only around the *D* and *D** masses smeared by the detector's momentum resolution. If the detected *D* is the result of *D** decay, the distribution in effective recoil mass observed is more complicated. The shape of the distribution then depends on the angular distribution of the decay *D* about the direction of motion of the parent *D**. Using angular momentum conservation, one can show that in reaction (2) the production angular distribution of the *D* meson with respect to the *D** helicity axis is of the form $dN/d\Omega \sim 1 + \alpha \cos^2\Theta$, with $\alpha = +1$ for $D^* \rightarrow \gamma D$ and $\alpha = -1$ for $D^* \rightarrow \pi D$. For reaction (3), the angular distribution is again of the form $dN/d\Omega \sim 1 + \alpha \cos^2\Theta$ if *F*

wave production is ignored. The parameter α is not calculable in (3) as it depends on the ratio of the ^1P and ^5P production amplitudes, and also on the decay mode of the undetected *D**.

The rates for reactions (1)—(3) were determined by fitting[19] the recoil-effective-mass-squared spectrum in two ways. The first method assumed that the angular distribution of a *D* relative to the direction of motion of its parent *D** was isotropic in reaction (3). The second method allowed for an angular dependence of the form

$$\frac{dN}{d\Omega} \sim 1 + \alpha \cos^2\Theta$$

as mentioned earlier, where α was determined by the fitting program for reaction (3). The angular dependence was assumed to be energy independent, but different α's were allowed for the different decay modes of the *D**. It was also assumed that the intermediate photon produced in the e^+e^- annihilation coupled directly to the $c\bar{c}$ quark pair which produced the observed *D* meson. Since that implies the *D*'s are in a pure isospin-zero state, the cross sections are related by

$$\sigma_{D^0\bar{D}^0} = \sigma_{D^+D^-} \left[\frac{p_{D^0}}{p_{D^+}} \right]^3 ,$$

$$\sigma_{D^{*0}\bar{D}^0} = \sigma_{D^{*+}D^-} \left[\frac{p_{D^0}}{p_{D^+}} \right]^3 ,$$

$$\sigma_{D^{*0}\bar{D}^{*0}} = \sigma_{D^{*+}D^{*-}} \left[\frac{p_{D^{*0}}}{p_{D^{*+}}} \right]^3 .$$

The p^3 factors account for phase-space differences in the production of charged and neutral *D*'s produced in $l = 1$ states. Finally, it was assumed that

TABLE II. Definition of variables appearing in the fitting functions.

Variable	Definition
L	Integrated luminosity of data sample.
$\epsilon_{K\pi}(M_R^2)$	Momentum-dependent detection efficiency for $D^0 \rightarrow K^- \pi^+$ from Fig. 2.
$\epsilon_{K\pi\pi}(M_R^2)$	Momentum-dependent detection efficiency for $D^- \rightarrow K^+ \pi^- \pi^-$ from Fig. 2.
$B(D^0 \rightarrow K^- \pi^+)$	Branching fraction for $D^0 \rightarrow K^- \pi^+ = 0.03 \pm 0.006$.
$B(D^+ \rightarrow K^+ \pi^+ \pi^+)$	Branching fraction for $D^+ \rightarrow K^- \pi^+ \pi^+ = 0.063 \pm 0.011$.
$B(D^* \rightarrow X)$	Branching fraction for *D** decay to state *X*.
ΔM_R^2	Bin width of data in dN/dM_R^2 distribution.

$$B(D^{*+} \rightarrow D^0\pi^+) + B(D^{*+} \rightarrow D^+\pi^0)$$
$$+ B(D^{*+} \rightarrow D^+\gamma) = 1 \ ,$$
$$B(D^{*0} \rightarrow D^0\pi^0) + B(D^{*0} \rightarrow D^0\gamma) = 1 \ .$$

The expected distribution of D's was convoluted with detector resolution to obtain the fitting functions for neutral and charged D's as

$$dN^0 = L\Delta M_R^2 \epsilon_{K\pi}(M_R^2)B(D^0 \rightarrow K^-\pi^+)\left\{ 2\sigma_{D^0\bar{D}^0} + \sigma_{D^*\bar{D}^0}\left[C_2^0 + B(D^{*0} \rightarrow D^0\pi^0)C_1^0 + B(D^{*0} \rightarrow D^0\gamma)C_4^0 \right.\right.$$

$$\left. + B(D^{*+} \rightarrow D^0\pi^+)C_3^0 \left[\frac{p_{D^+}}{p_{D^0}^3} \right]^3 \right]$$

$$+ 2\sigma_{D^{*0}\bar{D}^{*0}}\left[B(D^{*0} \rightarrow D^0\pi^0)C_5^0 + B(D^{*0} \rightarrow D^0\gamma)C_7^0 \right.$$

$$\left.\left. + B(D^{*+} \rightarrow D^+\pi^0)C_6^0 \left[\frac{p_{D^{*+}}}{p_{D^{*0}}} \right]^3 \right]\right\} + Q^0 \ ,$$

$$dN^+ = L\Delta M_R^2 \epsilon_{K\pi\pi}\left\{ 2\sigma_{D^0\bar{D}^0}\left[\frac{p_{D^+}}{p_{D^0}} \right]^3 C_0^+ + \sigma_{D^{*0}\bar{D}^0}\left[\frac{p_{D^+}}{p_{D^0}} \right]^3 [B(D^{*+} \rightarrow D^+\gamma)C_3^+ + B(D^{*+} \rightarrow D^+\pi^0)C_1^+ + C_2^+] \right.$$

$$\left. + 2\sigma_{D^{*0}\bar{D}^{*0}}\left[\frac{p_{D^{*+}}}{p_{D^{*0}}} \right]^3 [B(D^{*+} \rightarrow D^+\gamma)C_4^+ + B(D^{*+} \rightarrow D^+\pi^0)C_5^+] \right\} + Q^+ \ ,$$

TABLE III. Recoil-mass distribution dN/dM_R^2. Each distribution is normalized to unity when integrated over the possible kinematic range. Each process refers to the charge-conjugate process as well. For ease in defining the distributions, a D^0 is the detected particle in all the C^0 distributions and a D^+ is the detected particle in the C^+ distributions.

Distribution	Event type
C_0^0	$e^+e^- \rightarrow D^{*0}\bar{D}^0$
C_1^0	$e^+e^- \rightarrow D^{*0}\bar{D}^0, \ D^{*0} \rightarrow D^0\pi^0$
C_2^0	$e^+e^- \rightarrow D^0\bar{D}^{0*}$
C_3^0	$e^+e^- \rightarrow D^{*+}D^-, \ D^{*+} \rightarrow D^0\pi^+$
C_4^0	$e^+e^- \rightarrow D^{*0}\bar{D}^0, \ D^{*0} \rightarrow D^0\gamma$
C_5^0	$e^+e^- \rightarrow D^{*0}D^{*0}, \ D^{*0} \rightarrow D^0\pi^0$
C_8^0	$e^+e^- \rightarrow D^{*+}D^{*-}, \ D^{*+} \rightarrow D^0\pi^+$
C_7^0	$e^+e^- \rightarrow D^{*0}\bar{D}^{*0}, \ D^{*0} \rightarrow D^0\gamma$
C_0^+	$e^+e^- \rightarrow D^+D^-$
C_1^+	$e^+e^- \rightarrow D^{*+}D^-, \ D^{*+} \rightarrow D^+\pi^0$
C_2^+	$e^+e^- \rightarrow D^+D^{*-}$
C_3^+	$e^+e^- \rightarrow D^{*+}D^-, \ D^+\gamma$
C_4^+	$e^+e^- \rightarrow D^{*+}D^{*-}, \ D^{*+} \rightarrow D^+\gamma$
C_5^+	$e^+e^- \rightarrow D^{*+}D^{*-}, \ D^{*+} \rightarrow D^+\pi^0$

where Q^0 and Q^+ are quadratic parametrizations of the backgrounds and the other parameters are defined in Tables II and III. To check this fitting function, a Monte Carlo model was constructed which generated reactions (1), (2), and (3) and the subsequent D^* decays according to the matrix elements given by Cahn and Kayser.[20] The distribution of neutral D's produced by the Monte Carlo model at a center-of-mass energy of 4.16 GeV is shown in Fig. 10 together with the function fitted to the recoil-mass-squared distribution. The fitting procedure accurately reproduced the input parameters of the Monte Carlo model.

To increase the statistical accuracy of the fitting procedure, a simultaneous χ^2 minimization was done to eight different data sets. These consisted of the recoil-mass-squared spectra opposite both charged and neutral D's in the four center-of-mass energy regions $3.88 \leq E_{c.m.} \leq 4.02$ GeV, $4.02 \leq E_{c.m.} \leq 4.15$ GeV, $E_{c.m.} = 4.16$ GeV, and $4.15 \leq E_{c.m.} \leq 4.3$ GeV exclusive of the 4.16 GeV data.

The results of this fitting are given in Tables IV and V and shown for the isotropic fit to the data from 4.02 to 4.15 GeV in Fig. 11. The fact that
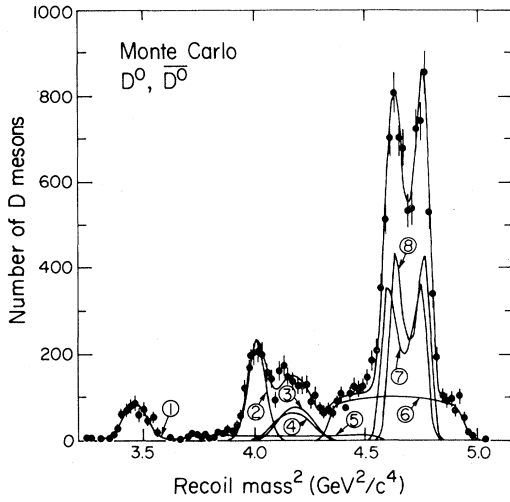
FIG. 10. The Monte Carlo—produced recoil-mass-squared spectrum produced opposite a detected neutral *D* at a center-of-mass energy of 4.16 GeV. The uppermost curve is a fit to the spectrum using the fitting function described in the text. The numbered curves show contributions from the processes (1) $D^0\bar{D}^0$, (2) $D^0\bar{D}^{0*}$, (3) $D^{*+}D^-$, $D^{*+}\rightarrow D^0\pi^+$, (4) $D^{*0}\bar{D}^0$, $D^{*0}\rightarrow D^0\pi^0$, (5) $D^{*0}\bar{D}^0$, $D^{*0}\rightarrow D^0\gamma$, (6) $D^{*0}\bar{D}^{*0}$, $D^{*0}\rightarrow D^0\gamma$, (7) $D^{*0}\bar{D}^{*0}$, $D^{*0}\rightarrow D^0\pi^0$, and (8) $D^{*+}D^{*-}$, $D^{*+}\rightarrow D^0\pi^+$. The double peak near 4.6 GeV^2/c^4 is a consequence of the angular distribution of the D^0 with respect to the D^* helicity axis.

the results of the anisotropic and isotropic fits are nearly identical indicates that the results obtained are relatively insensitive to the exact form of the production matrix element. As a consistency check, the inclusive value of R_D from Sec. III is compared with the value of R_D obtainable from

Table IV. The comparison of these cross sections is shown in Table VI. The value of R_D resulting from the exclusive channel analysis requires that R_D be the result of reactions (1), (2), and (3), only. The good agreement between the two methods indicates that the background parametrization used in the exclusive channel fits is reasonable, especially since the two methods for determining the background were completely independent. In the inclusive analysis, the background was determined from the shape of the *D* invariant-mass spectrum in D^0 or $\bar{D}^0 \rightarrow K\pi$ and $D^\pm \rightarrow K\pi^\pm\pi^\pm$ while for the exclusive decays, the background determination came entirely from the parametrization of the recoil-mass spectrum opposite the *D*. The branching ratios for D^* decay determined by the fit are shown in Table V and are in good agreement with the previously reported Mark I results.[1]

Soon after the discovery of the *D* it was suggested that the relative ratios of reactions (1), (2), and (3) could be described by simply counting the number of spin states available to each reaction.[21] This reasoning predicts the relative ratios of these reactions as

$$\sigma_{D\bar{D}}:\sigma_{D^*\bar{D}}:\sigma_{D^*\bar{D}^*} = p_{D,\bar{D}}{}^3:4p_{D^*,\bar{D}}{}^3:7p_{\bar{D}^*,\bar{D}}{}^3 .$$

At a center-of-mass energy of 4.16 GeV, this argument predicts the ratio 1:2.2:1.45 in contrast to the experimentally observed ratio of $(1.0\pm0.6):(4.6\pm1.2):(9.8\pm1.6)$. A way to explain this ratio by introducing dynamical arguments has been presented by Eichten *et al.*[22] They postulate production of quark-antiquark pairs, attracted by a potential of the form $V(r) = -k/r + r/a^2$ where *r*

TABLE IV. Two-body cross sections from recoil-mass fits.

Cross section (nb)	Energy region			
	3.88 — 4.02 GeV	4.02 — 4.15 GeV	4.16 GeV	4.15 — 4.3 GeV
	Isotropic fit			
$\sigma_{D\bar{D}}$	$0.2^{+0.3}_{-0.2}$	0.3 ± 0.3	0.4 ± 0.2	0.3 ± 0.3
$\sigma_{D^*\bar{D}}$	2.7 ± 0.7	3.8 ± 0.6	2.0 ± 0.4	1.6 ± 0.5
$\sigma_{D^*\bar{D}^*}$		5.7 ± 0.8	4.4 ± 0.6	3.1 ± 0.6
	Anisotropic fit			
$\sigma_{DD'}$	$0.2^{+0.3}_{-0.2}$	$0.2^{+0.3}_{-0.2}$	0.4 ± 0.3	0.3 ± 0.3
$\sigma_{D^*\bar{D}}$	2.6 ± 0.7	3.7 ± 0.7	2.0 ± 0.5	1.6 ± 0.5
$\sigma_{D^*\bar{D}^*}$		5.9 ± 1.2	4.4 ± 0.7	3.2 ± 0.8

TABLE V. Branching ratios from recoil-mass fits.

Mode	Isotropic fit	Anisotropic fit	Mark I result
$D^{*0} \rightarrow D^0 \pi^0$	0.47 ± 0.09	0.53 ± 0.12	0.55 ± 0.15
$D^{*0} \rightarrow D^0 \gamma$	0.53 ± 0.09	0.47 ± 0.12	0.45 ± 0.15
$D^{*+} \rightarrow D^0 \pi^+$	0.44 ± 0.07	0.44 ± 0.10	0.60 ± 0.15
$D^{*+} \rightarrow D^+ \pi^0$	0.28 ± 0.07	0.34 ± 0.07	
$D^{*+} \rightarrow D^+ \gamma$	0.28 ± 0.10	0.22 ± 0.12	

is the $q\bar{q}$ separation. Rates were calculated according to nonrelativistic quantum-mechanical rules assuming that the virtual photon produced in e^+e^- annihilation couples directly to the c-$\bar{c}$ pair. The model parameters are determined from the observed charmonium states. Figure 12 shows the predictions of this model for the energy dependence of the cross sections which describe reactions (1), (2), (3). Overplotted are the results of the isotropic fit given in Table II for these reactions. The relative magnitudes observed are in approximate

agreement with this model. $D\bar{D}$ production is suppressed at all energies while $D^*\bar{D}^*$ production accounts for the bulk of observed D's over the entire center-of-mass energy region from 3.9 to 4.3 GeV. Agreement between the model and the observed $D\bar{D}$ and $D^*\bar{D} + \bar{D}^*D$ production cross sections is good in all four energy bins.

VII. SUMMARY AND CONCLUSION

The D-meson production cross section has been measured at center-of-mass energies between 3.88 and 6.7 GeV. The comparison of this cross section to the total hadronic cross section leads one to conclude that D production accounts for almost all the charm contribution to the total hadronic cross section in this energy region. Over the limited kinematic range available, the inclusive differential cross section $s\, d\sigma/dz$ at 5.2 GeV is well described by the simple parametrization $s\, d\sigma/dz = A(1-z)^n$ with $n = 0.9 \pm 0.4$. No evidence was found for the associated production of charmed mesons and charmed baryons at 5.2 GeV. An upper limit for this cross section is 0.4 nb at the 90% confidence level. The energy dependences of the quasi-two-body production cross sections $\sigma_{D\bar{D}}$, $\sigma_{D^*\bar{D}}$, and $\sigma_{D^*\bar{D}^*}$ were measured between 3.88 and 4.3 GeV. The exclusive two-body cross sections were found to have an energy dependence which is in reasonable agreement with the dependence predicted by
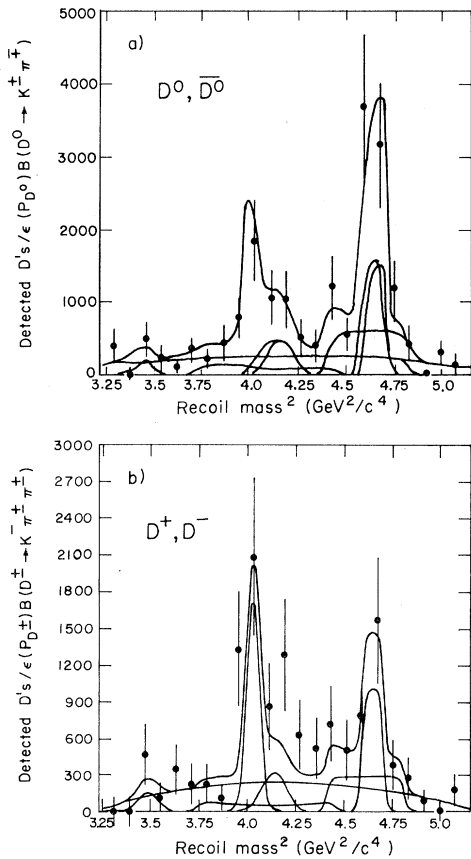

FIG. 11. Two of the eight recoil spectra simultaneously fit using the recoil distribution function described in the text. The data shown were taken at center-of-mass energies between 4.02 and 4.15 GeV.

TABLE VI. Comparison of inclusive D cross section (before radiative corrections) obtained from invariant-mass fits and those obtained from recoil-mass fits.

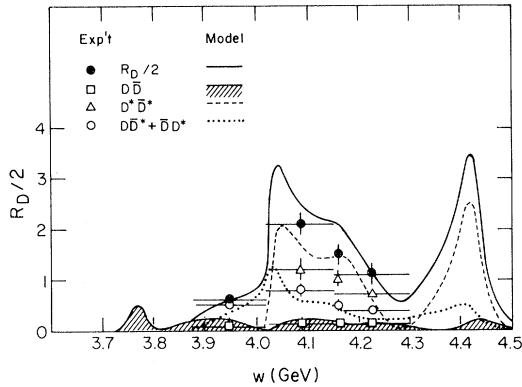| Energy region (GeV)	Recoil method (nb)	Inclusive method (nb)
3.88 − 4.02	2.9 ± 0.8	4.9 ± 1.3
4.02 − 4.15	9.8 ± 1.0	9.4 ± 1.0
4.16	6.8 ± 0.7	6.5 ± 0.7
4.15 − 4.30	5.1 ± 1.0	5.7 ± 1.4

FIG. 12. Comparison of the energy dependence of the exclusive *D* production cross sections observed to that predicted by the model of Eichten *et al.*[22]

Eichten *et al.*[22] as a dynamical consequence of a quark-antiquark binding potential. The branching fractions for *D** decay to *Dπ* and *Dγ* were found to be in agreement with previous results.[10]

ACKNOWLEDGMENTS

(a)Present address: Carnegie-Mellon University, Pittsburgh, PA 15213.
(b)Present address: Harvard University, Cambridge, MA 02138.
(c)Present address: DESY, Hamburg, Federal Republic of Germany.
(d)Present address: LPNHE Ecole Polytechnique, Palaiseau, France.
(e)Present address: Vanderbilt University, Nashville, TN 37235.
(f)Present address: EP Division, CERN, Geneva, Switzerland.
(g)Present address: California Institute of Technology, Pasadena, CA 91125.
(h)Present address: CEN-Saclay, France.
(i)Present address: Universitat Bonn, Federal Republic of Germany.

[1]R. H. Schindler *et al.*, Phys. Rev. D <u>24</u>, 78 (1981).
[2]P. A. Rapidis *et al.*, Phys. Rev. Lett. <u>39</u>, 526 (1977); H. F. W. Sadrozinski, in *High Energy Physics—1980*, proceedings of the XXth International Conference, Madison, Wisconsin, edited by L. Durand and L. G. Pondrom (AIP, New York, 1981).
[3]H. K. Nguyen *et al.*, Phys. Rev. Lett. <u>39</u>, 262 (1977).
[4]I. Peruzzi *et al.*, Phys. Rev. Lett. <u>39</u>, 1301 (1977).
[5]Reference 1 gives branching fractions for *D* decays. See also G. Abrams *et al.*, Phys. Rev. Lett. <u>43</u>, 481 (1979) and Ref. 4. Measurements of *D** branching fractions are given in Ref. 9.
[6]M. Piccolo *et al.*, Phys. Lett. <u>86B</u>, 220 (1979).
[7]W. Davies-White *et al.*, Nucl. Instrum. Methods <u>160</u>, 227 (1979).
[8]G. S. Abrams *et al.*, Phys. Rev. Lett. <u>43</u>, 477 (1979); G. S. Abrams *et al.*, *ibid.* <u>43</u>, 481 (1979).
[9]G. S. Abrams *et al.*, IEEE Trans. Nucl. Sci. <u>27</u>, 59 (1980).
[10]G. Goldhaber *et al.*, Phys. Lett. <u>69B</u>, 503 (1977).
[11]J. L. Siegrist, Ph.D thesis, Report No. SLAC-225, 1979 (unpublished); R. H. Schindler *et al.*, Phys. Rev.

D <u>21</u>, 2716 (1980).
[12]G. Bonneau and F. Martin, Nucl. Phys. <u>B27</u>, 381 (1971).
[13]J. Burmester *et al.*, Phys. Lett. <u>66B</u>, 395 (1977); R. Brandelik *et al.*, *ibid.* <u>76B</u>, 361 (1978); and J. Kirkby *et al.*, in *Weak Interactions—Present and Future*, proceedings of the SLAC Summer Institute on Particle Physics, 1978, edited by M. Zipf (SLAC, Stanford, 1978); J. L. Siegrist *et al.*, Phys. Rev. D <u>26</u>, 969 (1982).
[14]G. S. Abrams *et al.*, Phys. Rev. Lett. <u>44</u>, 10 (1980).
[15]We have attempted to determine the number of particles produced in association with the two *D* mesons at 5.2 GeV by comparing the produced charged-particle multiplicity distribution observed opposite a *D* candidate at this energy with the distribution observed at 3.77 GeV. The distribution at 5.2 GeV contains a very large uncertainty due to background subtractions causing the comparison of the distributions to be of little statistical significance.
[16]V. Luth *et al.*, Phys. Rev. Lett. <u>70B</u>, 120 (1977); V. Luth, in *Quark Spectroscopy and Hadron Dynamics*, proceedings of the SLAC Summer Institute on Particle Physics, 1977, edited by M. Zipf (SLAC, Stanford, 1977); G. Hanson, in *Gauge Theories and Leptons*, proceedings of the 13th Rencontre de Moriond, Les Arcs, Savoie, France, 1978, edited by Trân Tranh Vân (Editions Frontieres, Gif-sur-Yvette, 1979).
[17]P. A. Rapidis *et al.*, Phys. Lett. <u>84B</u>, 507 (1979). See also Ref. 6.
[18]The branching ratio determined by Mark II for $D^0 \rightarrow K^-\pi^+\pi^-\pi^+$ from Ref. 1 was used in this calculation: $B(D^0 \rightarrow K^-\pi^+\pi^-\pi^+) = (8.5\pm2.1)\%$.
[19]Further details of the fitting procedure are given in M. Coles, Ph.D. thesis, Report No. LBL-11513, 1980 (unpublished).
[20]R. Cahn and B. Kayser, Phys. Rev. D <u>22</u>, 2752 (1980).
[21]F. E. Close, Phys. Lett. <u>65</u>, 55 (1976).
[22]E. Eichten *et al.*, Phys. Rev. D <u>21</u>, 203 (1980).